

# MONSOON FLOODING RESPONSE: A MULTI-SCALE APPROACH TO WATER-EXTENT CHANGE DETECTION

Marco Gianinetto <sup>\*,(a)</sup>, Paolo Villa <sup>(b)</sup>

**DIAR-Remote Sensing Laboratory**, Politecnico di Milano University, Piazza Leonardo da Vinci 32, 20133 Milano, Italy – (marco.gianinetto, paolo.villa)@polimi.it

<sup>(a)</sup> Commission III, WG III/1, Commission VII, WG VII/6, Commission VIII, WG VIII/2

<sup>(b)</sup> Commission VII, WG VII/5

**KEY WORDS:** Flood map, Disaster Response, Change Detection, Multi resolution, Principal Components Transform, DEM

## ABSTRACT:

This paper has the aim of illustrating an automatic and speditive way for retrieving inundation extent from multispectral and multitemporal satellite data, together with land-cover changes caused by flooding events, which is a fundamental issue for managing a reconstruction plan after the event. A straightforward method to map inundated areas was applied in the North-Eastern region of Bangladesh, heavily struck by monsoonal rains in September 2000. This method is based on the Principal Components Transform (PCT) of multispectral satellite data, in its Spectral-Temporal implementation, followed by logical filtering and image segmentation, in order to reach the needed coherency of the results. The use of multiresolution data (28.5-meters ground resolution Landsat-7/ETM+ and 1,100-meters ground resolution NOAA-14/AVHRR) makes possible to evaluate hazard affected areas at different scales. Comparison to RADARSAT-derived water extension maps assessed an Overall Accuracy between 86.4% (for the flood map derived with NOAA-14/AVHRR data over the whole Bangladesh) and 90.6% (for the flood map derived with Landsat-7/ETM+ data over the North-East part of the country).

## 1. INTRODUCTION

During the last decades, satellite Remote Sensing has provided not only a systematic framework for scientific knowledge of planetary dynamics, at various scales, but also an effective basis for better informed decision making, regarding issues ranging from planning to forecast and response to natural hazards (Brivio *et al.*, 2002).

Today, geospatial products derived with Remote Sensing techniques can address requirements of policy-support systems, at local, regional and also global scale. As regards flood hazards, a variety of tools, methods and platforms are available for evaluating rapid response strategies in areas affected by severe weather events: inundations, river floods, flash floods. Several studies compose the literature of Remote Sensing flood analysis, through the use of: Synthetic Aperture Radar (SAR) sensors which are little influenced by weather conditions (Imhoff *et al.*, 1987; Hess *et al.*, 1995; Pope *et al.*, 1997; Melack and Wang, 1998; Miranda *et al.*, 1998; Smith *et al.*, 1996), low-resolution sensors which are especially suitable for large areas mapping, thanks to their high revisit time (Berg *et al.*, 1981; Barton and Bathols, 1989; Anderson, 2002), and new high-resolution sensors which are very useful for local scale analysis (Bryant and Gilvear, 1999; Van Der Sande, *et al.*, 2003).

This paper illustrates an automatic and straightforward technique for retrieving inundation maps from multispectral and multitemporal satellite data, together with land cover changes caused by flooding events. The method developed by the authors has already proven to be very effective in isolating flooded areas (at peak level) from non-flooded areas over hilly regions at temperate mid-latitudes (Gianinetto *et al.*, 2006) and is now tested on a tropical region (Bangladesh).

Bangladesh is the country that suffer the most the effects of global warming process: in fact, it is a tropical country with extremely low average terrain elevation above the Mean Sea Level (MSL), that is to say it is directly and dangerously subject to the worst consequences of the rising in sea level (Sanyal and Lu, 2004). Moreover, Bangladesh, with India and the countries of the Indochinese peninsula, is an overcrowded country periodically affected by South Asia monsoon, which brings heavy rains and large floodings over the densely inhabited and cultivated plains of the region.

The aim of the method described is to supply political institutions (especially in less developed countries) with a rapid response, effective, prompt and as inexpensive as possible tool, in order to manage natural emergencies.

## 2. HYDROGRAPHY OF BANGLADESH

Bangladesh is a developing country covering an area of about 147,570 km<sup>2</sup>, located in South Asia between 20°34' and 26°38' North latitude and between 88°01' and 92°40' East longitude. At the northern and eastern borders it is surrounded by India, at the south-eastern part Myanmar is found and the southern part of the country is touched by the Bay of Bengal, part of the Indian Ocean. The hydrographical conformation of Bangladesh depends on the river network consisting of the Ganges, the Brahmaputra and the Meghna rivers with their tributaries, which flow through the country to the Indian Ocean, rising in the Himalaya mountains.

The main part of the country (about 80%) is composed of the floodplains of these three rivers, with very low elevations above the MSL, reaching 30 meters only in the extreme north-western

---

\* Corresponding author.

area and 1,000 meters in the hilly region along the north-eastern border.

The climate of Bangladesh, as in other parts of the Indian subcontinent, is severely influenced by the monsoon that originates over the Indian Ocean and carries warm, moist and unstable air. These monsoonal winds cause Bangladesh tropical climate, humid and warm, which is fairly uniform throughout the country.

The seasonal cycle is divided into three main periods: 1) a hot summer from March to June, with very high temperature and occasional rainfall; 2) a hot and humid monsoon from June to October, with heavy rainfall (about 80% of the total mean annual rainfall); and 3) a relatively cooler and drier winter from November to March. The mean annual rainfall varies in the country with the geographical location, ranging from 1,200 mm in the extreme west to 5,800 mm in the north-east. The average yearly rainfall is about 2,200 mm. The surface water system is dominated by the three major river systems: the Ganges-Padma, the Brahmaputra-Jamuna and the Meghna (MPO, 1991; Ahmad and Ahmed, 2003). Figure 1 shows a map of Bangladesh and of its major rivers.

Bangladesh is a predominantly rural country, with agriculture generating about 25% of the Gross Domestic Product (GDP) and employing about 63% of the labour force. The majority of households depends on economic primary activities. The country is one of the most densely populated in the world, with a population of 129.3 million of people and a density of 876 people per km<sup>2</sup> (MoF, 2001; Ahmad and Ahmed, 2003). The country is also one of the poorest, with about 59 million people classified as absolutely poor (45% of total population).

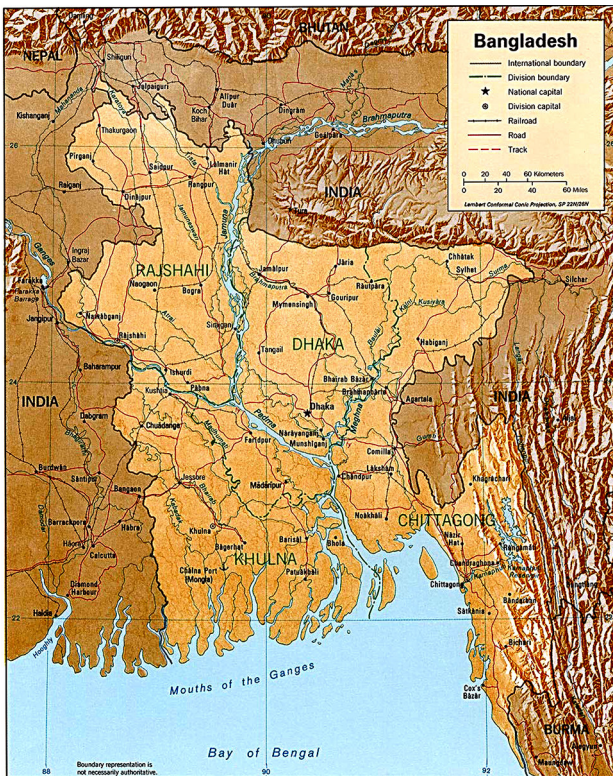


Figure 1. Map of Bangladesh focusing on relief and river system

The hydrographical, terrain, climatic and demographic characteristics of Bangladesh make this country severely prone to flooding events and suffering the most heavy damages done by floods to human life and environment.

### 3. CASE STUDY

The worst flood events in decades were those of 1998 and 2000. The end of summer of 1998 brought extreme monsoonal rains over Bangladesh and north-eastern India, causing massive floods over an area of nearly 70,000 km<sup>2</sup>. During the 80 days of duration for this event, 2,632 were the casualties, 25 million the homeless and displaced people, approximately 3,4 billion U.S. dollars the total value of damages; the numbers of a catastrophe (Anderson, 1998). The 2000 flood was less severe, but it struck a country already prostrated by the damages caused by the monsoonal event of two years before. This time the affected area reached 15,000 km<sup>2</sup>, the victims were 1,468 and the displaced about 24 million. The total esteemed damages exceeded 700 million U.S. dollars (Anderson, 2000).

This paper focus on the study of the 2000 flood: a 34 days long event that drowned much of the Indian border under 3 or more meters of water.

### 4. DATASET

The flood analysis has been performed using multisensor data (Landsat-7/ETM+ and NOAA-14/AVHRR) characterized by different spectral characteristics (six reflective spectral bands for Landsat-7/ETM+ and two reflective spectral bands for NOAA-14/AVHRR) and geometric resolutions (28.5 m ground resolution for Landsat-7/ETM+ and 1,100 m ground resolution for NOAA-14/AVHRR). Figures 2 and 3 illustrate in Colour InfraRed (CIR) visualization the study area at different scales: 1) regional scale for the NOAA-14/AVHRR data (Bangladesh country); and 2) local scale for the Landsat-7/ETM+ data (Haor region, in north-eastern Bangladesh).

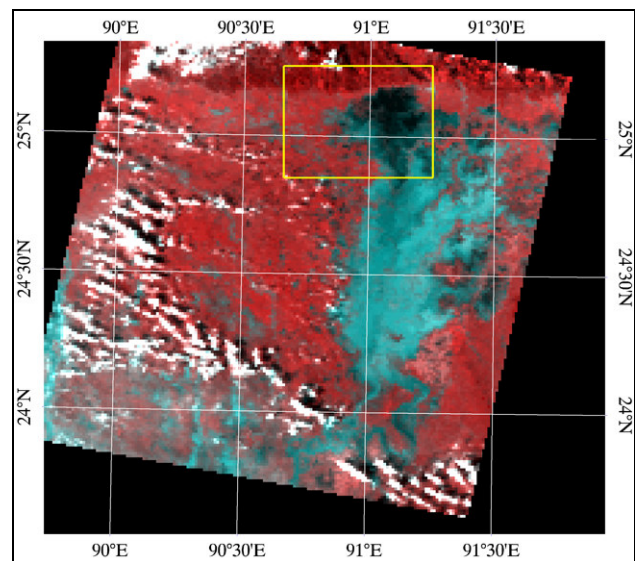


Figure 2. NOAA-14/AVHRR scene of Bangladesh (September 30, 2000 – post flood), showing the flooded area in the north-eastern region (CIR visualization: 2-1-1 band composition)

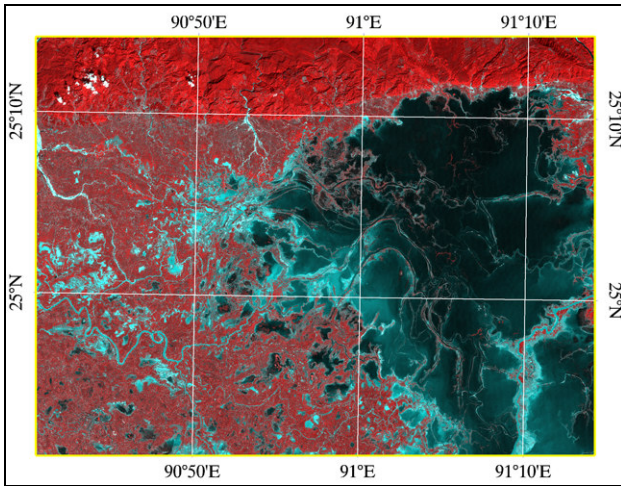


Figure 3. Landsat-7/ETM+ scene of north-eastern Bangladesh highlighted in the yellow rectangle in Figure 2 (October 25, 2000 – post flood), showing a detail of the flooded area in the Haor region (CIR visualization: 4-3-3 band composition)

In detail, data used are listed below:

- Two 1,100-meters NOAA-14/AVHRR HRPT images (Figure 2), centred at 24°29' North latitude and 90°41' East longitude:
  - 3 March, 2000 (pre flood)
  - 30 September, 2000 (post flood);
- Two 28.5-meters Landsat-7/ETM+ (Figure 3), centred at 25°03' North latitude and 90°57' East longitude:
  - 28 February, 2000 (pre flood)
  - 25 October, 2000 (post flood);
- 3-arcsec NASA Shuttle Radar Topography Mission (SRTM-v2) Digital Terrain Model (DTM), centred at 24°29' North latitude and 90°41' East longitude (WRS-2 p137 r43), with 1 m vertical resolution, and 16 m Linear Error at 90% confidence (LE90) vertical accuracy.

## 5. METHODOLOGY

Image pre-processing involved: 1) georeferencing; 2) atmospheric correction; and 3) synthetic images generation. Pre flood and post flood data (both NOAA-14/AVHRR and Landsat-7/ETM+) have been first georeferenced in the UTM-WGS84 F46N projection, using as Ground Control Points (GCPs) the ones provided with the satellite scenes and included in the metadata, obtaining a Root Mean Square Error (RMSE) over GCPs less than a quarter of image pixel. Then, atmospheric correction has been performed on raw data to retrieve ground reflectance, the physical quantity needed to compare multitemporal radiometric responses.

Atmospheric corrected reflectance images have been generated using a low resolution MODTRAN atmospheric model (Berk *et al.*, 1998), combined with aerosol retrieval based on band ratios and with correction for the adjacency effect on path radiance.

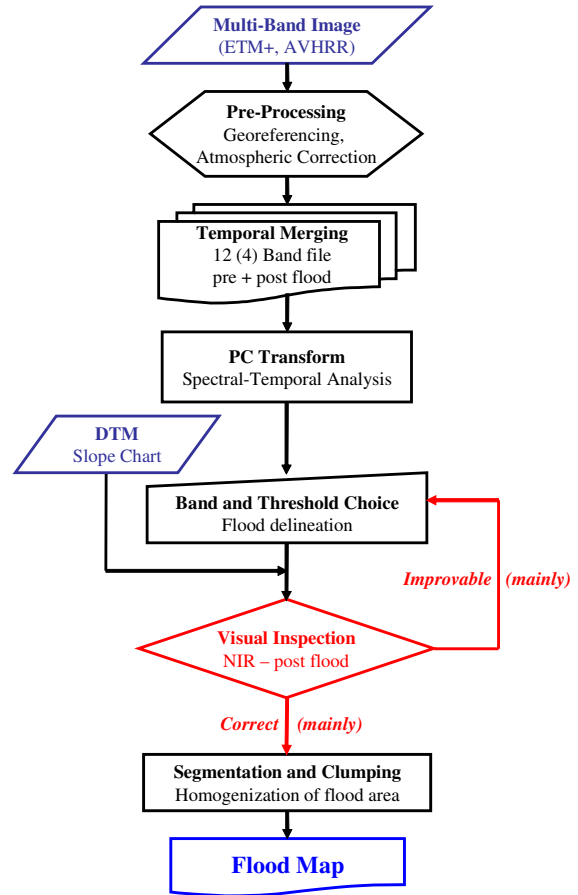


Figure 4. Flowchart for the methodology for retrieving inundation maps

Once obtained ground reflectance, a synthetic file composed of twice the number of the original spectral bands has been created for both the Landsat-7/ETM+ and the NOAA-14/AVHRR dataset, listing first the reflective bands of the pre flood scene, and then the homologous bands of the post flood scene (four-band file for NOAA-14/AVHRR and twelve-band file for Landsat-7/ETM+).

The core of the flood mapping methodology here described is based on the well known Principal Components Transform (PCT), in its Spectral-Temporal implementation (Ingebritsen and Lyon, 1985; Fung and LeDrew, 1987; Schowengerdt, 1997). The PCT realize a linear transformation which turns a set of correlated variables (the original spectral bands) in a new set of standardized and uncorrelated variables (the Principal Components, PC), ordered in decreasingly with covariance matrix eigenvalues (related to the variance of each new variable), that is to say in increasing order of information content. Figure 4 shows the flowchart of the entire mapping technique.

In this processing, the PCT has been applied to the synthetic files created as described above. Figure 5 shows an example of the PCT (the first Principal Component – PC1) applied to the Landsat-7/ETM+ data collected over the Haor region (Bangladesh), where the dark tones of the PC image are associated to water content and soil moisture. The separability between flooded and non-flooded areas is clearly visible in Figure 5, both in the PC image and in the frequency histogram, where the distance between water-related features (lower peak

of frequencies located around PC value -0.2) and non-water features (higher peak of frequencies located around PC value 0.1) is evident.

To improve the geometric coherency of the flood maps, the final processing contemplates: 1) logical filtering; 2) image segmentation; and 3) clumping.

Using the slope chart derived from the NASA's DTM processing, PC values have been filtered by excluding from the classification all the image pixels characterized by a terrain slope higher than a selected threshold, considering unlikely that steep terrain sites were reached by flooding waters. An initial threshold was derived from the frequency histogram of the PC (see Figure 5), chosen as separation between flood and non-flood areas. Threshold refinement has then been performed with several tests, evaluating the performance of each one by comparing the image filtering with the photo-interpretation of the post flood CIR image.

As spatial characteristics of flooded areas are usually not much fragmented and homogeneous in extension, a final homogenisation has been obtained through the classical image segmentation and clumping techniques, in order to achieve a sufficient coherency in the final flood map.

## 6. RESULTS AND DISCUSSION

The resulting flood maps generated with the methodology described (Figures 6 and 7) were retrieved using maximum threshold values and PC selection for each sensor. For the NOAA-14/AVHRR dataset the following values have been used:

- a) Principal Component used for classification= PC3
- b) PC3 threshold < -0.02
- c) Terrain Slope threshold < 4%

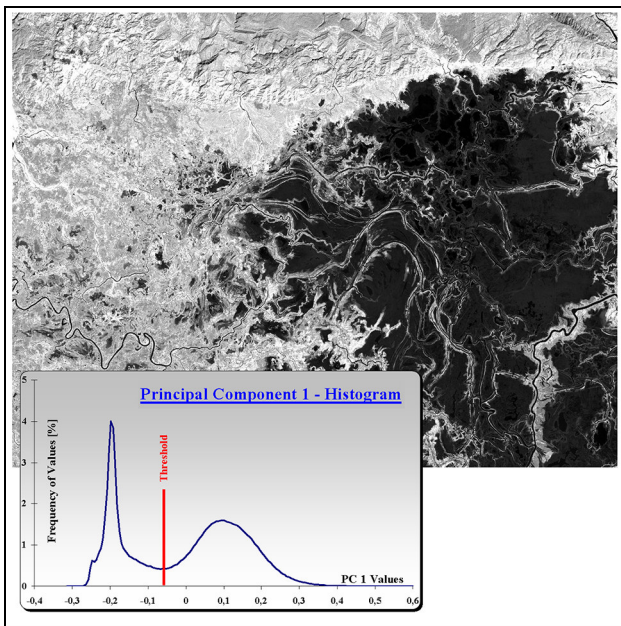


Figure 5. Spectral-Temporal Principal Component 1 of Landsat-7/ETM+ data, with superimposed the frequency histogram of the displayed values

While for the Landsat-7/ETM+ the following values have been used:

- a) Principal Component used for classification= PC1
- b) PC1 threshold < -0.06
- c) Terrain Slope threshold < 4%.

Both the conditions on PC threshold (a) and terrain slope threshold (b) have to be satisfied at the same time (logical AND).

In Figures 6 and 7 are displayed the flood maps derived for different scales and resolutions: blue areas in the images are representative of the maximum extent of water during the flood event, that is the flooded area at peak level. Figure 6 shows the flood map derived with NOAA-14/AVHRR data (1,100 m ground resolution) for a regional scale analysis, while Figure 7 shows the flood map derived with Landsat-7/ETM+ data (28.5 m ground resolution) in the north-eastern region of Bangladesh (Haor region) for a local scale analysis.

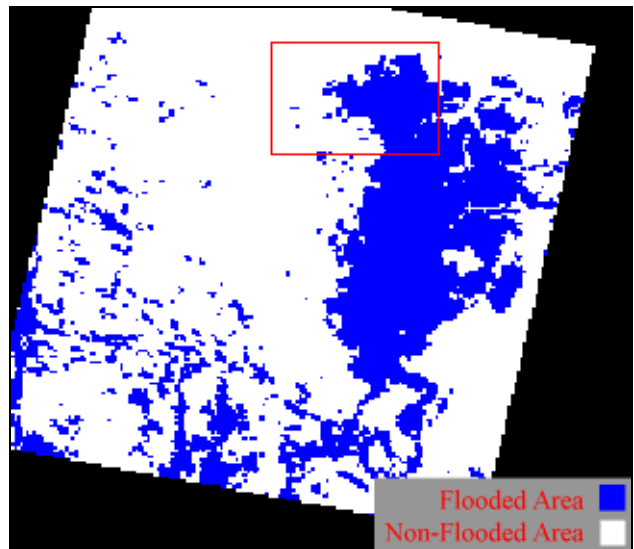


Figure 6. Flood map for the 2000 event in Bangladesh derived with NOAA-14/AVHRR data (1,100 m ground resolution).  
Regional scale analysis

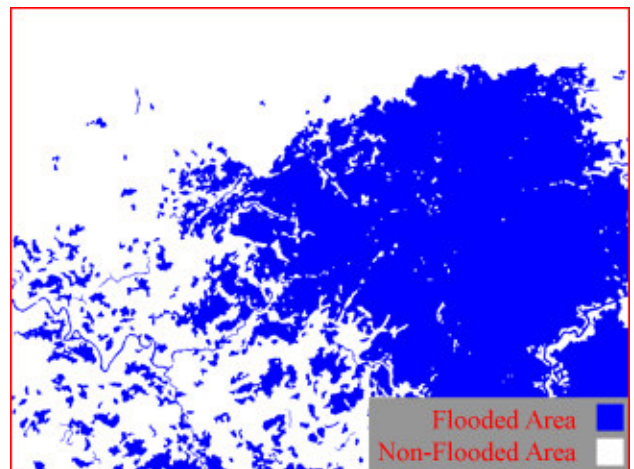


Figure 7. Flood map for the 2000 event in Bangladesh derived with Landsat-7/ETM+ data (28.5 m ground resolution). The classification refers the north-eastern region highlighted in the red rectangle of Figure 6. Local scale analysis

		Ground Truth		
		Flood	Non-Flood	Commission error (%)
Flood Map	Flood	4,962	2,235	31.05
	Non-Flood	1,352	17,853	7.04
	Omission error (%)	21.41	11.13	

Overall Accuracy = 86.41%  
Kappa Coefficient = 0.6437

Table 1. Confusion matrix for the flood map over the whole region derived from NOAA-14/AVHRR data

The differences in the PC selection are to be ascribed to the differences in spectral richness of NOAA-14/AVHRR data (only two reflective bands) and of Landsat-7/ETM+ data (six reflective bands). Moreover, the values of the PC thresholds are related to the land cover conditions of the analysed area, that is to say to its ground reflectance variability.

The accuracy of results has been tested using as ground truth a flood classification provided by Center for Environmental and Geographic Information Services (CEGIS), in form of water extent derived from RADARSAT data collected exactly on 30 September 2000 and on 25 October 2000, in coincidence with the acquisitions of the NOAA-14/AVHRR and of the Landsat-7/ETM+ post flood scenes, respectively. Tables 1 and 2 show the confusion matrixes for the classification maps derived from the NOAA-14/AVHRR and from the Landsat-7/ETM+ data, respectively, using as ground truth the CEGIS data.

As expected, the flood map derived with Landsat-7/ETM+ shows a higher accuracy than that of AVHRR-derived one. Once again, this is due to two main factors: 1) the higher geometric resolution of Landsat-7/ETM+ images (28.5 m), which results in more locally precise mapping of water extent (with lower omission and commission errors in the classification); and 2) the higher number of spectral bands for the Landsat-7/ETM+ (six reflective spectral bands), which ensures a better capability to discriminate spectral response of land cover objects, if compared with the two reflective bands of the NOAA-14/AVHRR.

## 7. CONCLUSIONS

Flood events are among the most frequent and dangerous hazards, causing thousands of casualties every year and producing millions of U.S. dollars of damages, especially in developing countries. Among less developed countries, Bangladesh is probably the one that suffer the most the enormous influence of extreme weather conditions, due to its geographic position in monsoon-afflicted south-asian region and to its hydrologic and terrain conformation.

This paper has focused on a straightforward and rapid method to retrieve inundation maps at different scales using remotely sensed satellite images, in order to provide decision makers with an efficient tool to plan a response strategy in the post flood phase of emergency and reconstruction. The method has proven not only rapid and direct, but also accurate (Overall Accuracy between 86.4% and 90.6% and Kappa Coefficient between 0.64 and 0.81) and, last but not least, less expensive than other methods, such as visual photo-interpretation and digitalization of aerial surveys, for example.

		Ground Truth		
		Flood	Non-Flood	Commission error (%)
Flood Map	Flood	1,214,410	149,842	10.98
	Non-Flood	132,117	1,503,631	8.08
	Omission error (%)	9.81	9.06	

Overall Accuracy = 90.60%  
Kappa Coefficient = 0.8103

Table 2. Confusion matrix for the flood map over the Haor region derived from Landsat-7/ETM+ data

The flood maps derived can be used to directly identify areas covered by water, but they could also be integrated in a GIS environment with demographic, infrastructural and land cover data, to produce a damage map for the flood event analysed. Moreover, the proposed multiscale approach shows how it is possible to analyse natural hazards of different extension and with different level of detail: from national level (to continental and even global scale) using low-resolution data with high revisit time (i.e. NOAA-14/AVHRR, but also Terra & Aqua/MODIS, ENVISAT/MERIS, or SPOT/VEGETATION), to regional and local scale using medium resolution data (i.e. Landsat-7/ETM+, but also SPOT/HRV-HRVIR or Terra & Aqua/ASTER).

## ACKNOWLEDGEMENTS

The present work owes a debt of gratitude to NASA sponsored Global Land Cover Facility (GLCF) of the University of Maryland for providing Landsat 7/ETM+ scenes over the Bangladesh (WRS-2 p137 r43), and to Dr. Mohammad Shahidul Islam of the Center for Environmental and Geographic Information Services (CEGIS), for providing the RADARSAT classified scenes, used for accuracy assessment.

## REFERENCES

### References from Journals:

- Ahmad, Q. K., Ahmed, A., U., 2003. Regional Cooperation in Flood Management in the Ganges-Brahmaputra Meghna Region: Bangladesh Perspective. *Natural Hazards*, 28, pp. 181-198.
- Barton, I. J., and Bathols, J. M., 1989. Monitoring floods with AVHRR. *Remote Sensing of Environment*, 30, pp. 89-94.
- Berk, A., Bernstein, L. S., Anderson, G. P., Acharya, P. K., Robertson, D. C., Chetwynd, J. H., and Adler-Golden, S. M., 1998. MODTRAN Cloud and Multiple Scattering Upgrades with Application to AVIRIS. *Remote Sensing of Environment*, 65(3), pp. 367-375.
- Brivio, P. A., Colombo, R., Maggi, M., and Tomasoni, R., 2002. Integration of remote sensing data and GIS for accurate mapping of flooded areas. *International Journal of Remote Sensing*, 23(3), pp. 429-441.
- Bryant, R. G., and Gilvear, D. J., 1999. Quantifying Geomorphic and Riparian Land Cover Changes Either Sides of a Large Flood Event Using Airborne Remote Sensing: River Tay, Scotland. *Geomorphology*, 29, pp. 307-321

Fung, T., and LeDrew, E., 1987. Application of principal component analysis to change detection. *Photogrammetric Engineering and Remote Sensing*, 53(12), pp. 1649-1658.

Gianinetto, M., Villa, P., and Lechi, G., 2006. Post-flood damage evaluation using Landsat TM and ETM+ data integrated with DEM. *IEEE Transactions on Geoscience and Remote Sensing*, 44(1), pp. 236-243.

Hess, L. L., Melack, J. M., Filoso, S., and Wang, Y., 1985. Realtime mapping of inundation on the Amazon floodplain with the SIR-C/X-SAR synthetic aperture radar. *IEEE Transactions on Geoscience and Remote Sensing*, 33, pp. 896-904.

Imhoff, M. L., Vermillion, C., Story, M. H., Choudhury, A. M., and Gafoor, A., 1987. Monsoon flood boundary delineation and damage assessment using spaceborne imaging radar and Landsat data. *Photogrammetric Engineering and Remote Sensing*, 4, pp. 405-413.

Ingebritsen, S. E., and Lyon, R. J. P., 1985. Principal components analysis of multitemporal image pairs. *International Journal of Remote Sensing*, 6, pp. 687-696.

Melack, J. M., and Wang, Y., 1998. Delineation of flooded area and flooded vegetation in Balbina Reservoir (Amazonas, Brazil) with synthetic aperture radar. *Verhandlungen Internationale Vereinigung für Limnologie*, 26, pp. 2374-2377.

Miranda, F. P., Fonseca, L. E. N., and Carr, J. R., 1998. Semivariogram textural classification of JERS-1 (Fuyo-1) SAR data obtained over a flooded area of the Amazon rainforest. *International Journal of Remote Sensing*, 19, pp. 549-556.

Pope, K. O., Rejmankova, E., Paris, J. F., and Woodruff, R., 1997. Detecting seasonal flooding cycles in marshes of the Yucatan Peninsula with SIR-C polarimetric radar imagery. *Remote Sensing of Environment*, 59, pp. 157-166.

Sanyal, J., and Lu X., X., 2004. Application of the Remote Sensing in Flood Management with Special Reference to Monsoon Asia: a Review. *Natural Hazards*, 33, pp. 283-301.

Smith, L. C., Bryan, L., and Bloom, A. L., 1996. Estimation of discharge from three braided rivers using synthetic aperture radar satellite imagery: potential application to ungauged basins. *Water Resources Research*, 32, pp. 2021-2034.

Van Der Sande, C. J., De Jong, S. M., and De Roo, A. P. J., 2003. A segmentation and Classification Approach of IKONOS-2 imagery for Land Cover Mapping to Assist Flood Risk and Flood Damage Assessment. *International Journal of Applied Earth Observation and Geoinformation*, 4, pp. 217-229

#### References from Books:

Berg, C. P., Matson, M., and Wiesnet, D. R., 1981. *Assessing the Red River of the North 1978 flooding from NOAA satellite data. Satellite Hydrology*. American Water Resources Association, Deutsch, M., Wiesnet D. R., and Rango, A. Eds., Minneapolis, pp. 309-315.

Schowengerdt, R. A., 1997. *Remote Sensing-Models and methods for image processing. Second Ed.* Academic Press.

#### References from websites:

Anderson, E., 2002. MODIS 250 Image Map Series of Western Tennessee with Inundation Maps, DFO-2001-147, Dartmouth

Flood Observatory, Hanover, USA, digital media, <http://www.dartmouth.edu/~floods/images/2001-147b.html> (accessed 28 Jan. 2006).

Anderson, E., 2000. Inundation Maps based on AVHRR 4km data from September 24, 2000, DFO-2000-061, Dartmouth Flood Observatory, Hanover, USA, digital media, <http://www.dartmouth.edu/~floods/2000061.html> (accessed 30 Mar. 2006).

Anderson, E., 1998. Satellite-Based Flood Analysis Map – India, Bangladesh and Tibet, DFO-1998-099, Dartmouth Flood Observatory, Hanover, USA, digital media, <http://www.dartmouth.edu/~floods/98099.jpg> (accessed 30 Mar. 2006).

#### References from Other Literature:

MoF, 2001. Bangladesh Economic Review 2001. Ministry of Finance (MoF), GoB, June 2001, Dhaka, Bangladesh.

MPO, 1991. National Water Plan, Master Plan Organization for Ministry Irrigation, Water Development and Flood Control, GoB, Dhaka, Bangladesh.